Per- and polyfluoroalkyl substance (PFAS) retention by colloidal activated carbon (CAC) using dynamic column experiments☆

Georgios Niarchos [a,*], Lutz Ahrens [b], Dan Berggren Kleja [c], Fritjof Fagerlund [a]

[a] *Department of Earth Sciences, Uppsala University, P.O. Box 256, SE-751 05, Uppsala, Sweden*
[b] *Department of Aquatic Sciences and Assessment, Swedish University of Agricultural Sciences (SLU), P.O. Box 7050, SE-750 07, Uppsala, Sweden*
[c] *Department of Soil and Environment, Swedish University of Agricultural Sciences (SLU), P. O. Box 7090, SE-750 07, Uppsala, Sweden*

ABSTRACT

Developing effective remediation methods for per- and polyfluoroalkyl substance (PFAS)-contaminated soils is a substantial step towards counteracting their widespread occurrence and protecting our ecosystems and drinking water sources. Stabilisation of PFAS in the subsurface using colloidal activated carbon (CAC) is an innovative, yet promising technique, requiring better understanding. In this study, dynamic soil column tests were used to assess the retardation of 10 classical perfluoroalkyl acids (PFAAs) (C_5–C_{11} perfluoroalkyl carboxylic acids (PFCAs) and C_4, C_6, C_8 perfluoroalkane sulfonates (PFSAs)) as well as two alternative PFAS (6:2 and 8:2 fluorotelomer sulfonates) using CAC at 0.03% w/w, to investigate the fate and transport of PFAS under CAC treatment applications. Results showed high retardation rates for long-chain PFAS and eight times higher retardation for the CAC-treated soil compared to the non-treated reference soil for the $\sum$PFAS. Replacement of shorter chain perfluorocarboxylic acids (PFCAs), such as perfluoropentanoic acid (PFPeA), by longer chained PFAS was observed, indicating competition effects. Partitioning coefficients (K_d values) were calculated for the CAC fraction at ~10^3–10^5 L kg^{-1} for individual PFAS, while there was a significant positive correlation ($p < 0.05$) between perfluorocarbon chain length and K_d. Mass balance calculations showed 37% retention of $\sum$PFAS in treated soil columns after completion of the experiments and 99.7% higher retention rates than the reference soil. Redistribution and elution of CAC were noticed and quantified through organic carbon analysis, which showed a 23% loss of carbon during the experiments. These findings are a step towards better understanding the extent of CAC's potential for remediation of PFAS-contaminated soil and groundwater and the limitations of its applications.

1. Introduction

Per- and polyfluoroalkyl substances (PFAS) are a vast chemical class of emerging occurrence and concern. Over decades, extensive use and uncontrolled disposal of PFAS have resulted in widespread environmental distribution (Zhao et al., 2012), with several PFAS detected in remote areas (Rankin et al., 2016) and pristine ecosystems (Filipovic et al., 2015). Soils have been identified as significant reservoirs and long-term sources of PFAS pollution, with concentrations reaching several hundred mg kg^{-1} at contaminated sites (Brusseau et al., 2020). PFAS occurrence in soils is typically due to fluoropolymer production facilities (Hoffman et al., 2011) and the application of aqueous film-forming foams (AFFFs), which subsequently results in groundwater contamination, as observed in the US (Nickerson et al., 2021; Weber et al., 2017), Canada (Liu et al., 2022), Australia (Bräunig et al., 2017), South Korea (Yong et al., 2021), and Sweden (Ahrens et al., 2014; Bergström, 2014). Highly prevalent novel and legacy PFAS in groundwater from AFFF-impacted sites include perfluorohexane sulfonic acid (PFHxS), perfluorooctane sulfonic acid (PFOS), perfluorohexanesulfone amide (PFHxSA), and 6:2 fluorotelomer sulfonic acid (6:2 FTSA) (Ahrens et al., 2014; Baduel et al., 2017; D'Agostino and Mabury, 2014; Place and Field, 2012). The infiltration of these PFAS into the subsurface is alarming, as it is estimated that at least half of the global population's drinking water sources depend on groundwater (Liu et al., 2019; Smith et al., 2016).

Several soil treatment approaches to counteract the PFAS soil contamination issue have become available in recent years. Often, they involve excavation of the soil and treatment *ex-situ* or disposal in

---

landfills (dig and dump) (Igor et al., 2021). However, these approaches can be problematic because they entail high costs and result in shifting the contamination from one place to another (Igor et al., 2021; Ross et al., 2018). Conversely, *in-situ* soil remediation at the source zones has been described as a sustainable and cost-effective treatment approach (Høisæter et al., 2021). In the case of PFAS, *in-situ* treatment includes destruction (e.g. chemical oxidation (Dombrowski et al., 2018), biodegradation (Huang and Jaffé, 2019)), removal (e.g. electrochemical removal (Niarchos et al., 2022; Sörengård et al., 2019), phytoremediation (Huang et al., 2021), soil flushing (Senevirathna et al., 2021)), and stabilisation or solidification (e.g. using biochar (Inyang and Dickenson, 2017), activated carbons (Sörengård et al., 2020), stabilisation/solidification (S/S) (Sörengård et al., 2021)) techniques. Stabilisation methods have been identified as the most mature and feasible techniques to-date (Ross et al., 2018). They typically involve the addition of fixation agents in the subsurface to prevent leaching from soils into groundwater. Stabilisation has also been shown to decrease the bioavailability of PFAS (Hearon et al., 2022), reducing their uptake in plants and other living organisms (Bolan et al., 2021).

Different materials have been used as fixation agents for PFAS treatment, such as natural clays and clay-biochar composites (Mukhopadhyay et al., 2021; Yao et al., 2014), various biochars (Kupryianchyk et al., 2016; Sørmo et al., 2021), and activated carbons (Du et al., 2014; Sorengard et al., 2019). Activated carbons come in various forms based on grain size, typically as granular (GAC, 0.4–1.2 mm) or powdered activated carbon (PAC, <1 mm). Colloidal activated carbon (CAC) is a novel material consisting of very fine particles (1–2 μm) and, consequently, a very large surface area. It has the added benefit that carbon particles are suspended in solution and can be injected in the subsurface, thus exhibiting ease of application in the field (McGregor, 2018).

Sorption of PFAS to activated carbons and their partitioning behaviour depend on their diverse molecular structure (polymeric, non-polymeric; neutral, anionic, cationic, zwitterionic; short-chain, long-chain). The main mechanisms for PFAS sorption include hydrophobic and oleophobic effects, electrostatic interactions, and interfacial behaviours, such as inner-sphere complexes (Du et al., 2014). The per-fluorocarbon chain length is reportedly one of the dominant factors for PFAS sorption, with long-chain PFAS referring to perfluoroalkyl carboxylic acids (PFCAs) with $C \geq 8$, perfluoroalkyl sulfonates (PFSAs) with $C \geq 6$, and all other PFAS with $C \geq 7$ (Buck et al., 2011). Adsorption capacity reportedly increases with increasing perfluoroalkyl chain length (Campos Pereira et al., 2018; Higgins and Luthy, 2006; Sepulvado et al., 2011); therefore, short-chain PFAS have a higher susceptibility to leaching. PFAS partitioning studies have so far mainly been conducted through batch tests, i.e. shaking tests to reach adsorption equilibrium (Qian et al., 2017; Son et al., 2020; Sorengard et al., 2019; Sørmo et al., 2021). Recently, the sorption of perfluorooctanoic acid (PFOA) and perfluorooctane sulfonic acid (PFOS) to soils was compared between batch and column tests, with both methods producing similar results (Van Glubt et al., 2021). However, the reported advantages of column tests were recognised, including the simulation of more realistic conditions and their usefulness to detect secondary transport phenomena (Van Glubt et al., 2021). Additionally, batch tests are unsuitable for investigating desorption phenomena and long-term retention. Maizel et al. (2021) studied the leaching of over one hundred PFAS from AFFF-impacted surface soils using column experiments and identified nonideal adsorption behaviour, denoting the complexity of PFAS transport. Other column studies have also exhibited non-equilibrium transport (Guelfo et al., 2020) and the significance of infiltration rates (Høisæter et al., 2019) in various soils. Still, the PFAS transport under CAC soil treatment remains largely unexplored.

In this context, the objective of this study was to investigate the transport behaviour of 12 PFAS in a soil treatment scenario with CAC, with the use of 1-D flow dynamic column experiments for the first time. The target PFAS included legacy perfluoroalkyl acids (PFAAs) and fluorotelomer sulfonates (FTSAs), which are highly relevant for AFFF-

impacted sites. The sorption of PFAS to soil and CAC was examined, followed by a desorption phase to assess the reversibility of the process. Furthermore, the study aimed to increase the understanding of CAC's behaviour in the subsurface by investigating its washing-out potential and distribution along the soil column.

2. Materials and methods

2.1. Chemicals and materials

The colloidal activated carbon used in the experiments was provided by Regenesis (PlumeStop®). According to the manufacturer, the specific surface area (SSA) of the CAC was 900 m² g⁻¹, the iodine number ≈ 1000 mg g⁻¹, its particle size 1–2 μm, and the ζ potential −80 to −2 mV at pH 7 and ionic strength of 1–500 mM (Regenesis, personal communication, 2022). The PFAS standards included in the study were all laboratory grade. Native PFAS standards included were perfluoropentanoic acid (PFPeA, Wellington Laboratories (>98%)), perfluorohexanoic acid (PFHxA, Wellington Laboratories (>98%)), perfluoroheptanoic acid (PFHpA, Wellington Laboratories (>98%)), perfluorooctanoic acid (PFOA, Wellington Laboratories (>98%)), perfluorononanoic acid (PFNA, Wellington Laboratories (>98%)), perfluorodecanoic acid (PFDA, Wellington Laboratories (>98%)), perfluoroundecanoic acid (PFUnDA, Wellington Laboratories (>98%))), C_4, C_6, C_8 perfluorosulfonic acids (PFSAs) (perfluorobutane sulfonic acid (PFBS, Wellington Laboratories (>98%)), PFHxS (Wellington Laboratories (>98%)), PFOS (Wellington Laboratories (>98%)), and 6:2 and 8:2 fluorotelomer sulfonic acids (FTSAs) (6:2 FTSA, 8:2 FTSA, Apollo Scientific Ltd (purity not available) (Table S1 in supporting information (SI)). Information on mass-labelled internal standards (IS) used for quantitation of native PFAS is presented in Table S2 in SI. The basic physicochemical properties of the target PFAS are presented in Table S3 in SI.

2.2. Soil sampling and preparation

Soil was sampled at a depth of approximately 3 m in central Sweden (59°23′13.7″N, 15°53′48.2″E). The sampling location was adjacent to a PFAS-contaminated site of interest. Based on initial screening, most of the target PFAS were below detection limits (Table S4 in SI). After sampling, the soil was air-dried for 10 days at 40 °C in a room sheltered from dust deposition, then ground with a mortar and pestle, sieved to remove large particles (>2 mm), and homogenised by shaking. The soil was a silt loam, with a relatively high amount of clay and fine silt particles, while it was low in organic carbon and PFAS (for details, see Tables S5 and S6 in SI). Before packing, the soil was mixed with premium #40/50 silica sand (AGSCO, USA) at 1:5 (field soil):(silica sand) ratio to increase the hydraulic conductivity of the columns. For the treated soil, CAC was added to the mixture at a final concentration of 0.031% w/w, based on manufacturer suggestions (Regenesis, personal communication, 2020).

2.3. Column design and packing

Column tests were conducted in custom-made transparent PVC pipes (soil chamber L = 15 cm, d = 3.6 cm) having a length to diameter ratio >4 to simulate field conditions and minimise transverse dispersivity (Banzhaf and Hebig, 2016; Gibert et al., 2012; Lewis and Sjöstrom, 2010). The flow was directed upward to facilitate the escape of entrapped air bubbles. Two chambers of gravel in the inlet and outlet of the columns were included to ensure uniform flow in the soil column (L = 2 cm, d = 3.6 cm), by increasing dispersion and avoiding flow convergence at the entrance and exit points. Nylon mesh (pore diameter = 50 μm) was placed at the inlet and outlet and secured in place with perforated PVC plates.

Packing of the columns aimed at a uniform matrix, saturated and free

of air bubbles. In total, four column experiments were conducted, with treated (T1, T2) and reference soil (R1, R2) tested in duplicates (Table 1). Preparation of soil columns followed the guidelines of Lewis and Sjöström (2010); thin layers of dry soil were deposited into the column from a few centimetres height and soil was saturated from the inflow while mixing the soil and vibrating the column to remove entrapped air. It has been reported that this technique can produce the highest uniformity of packing (Lewis and Sjöström, 2010). In total, 306 $\pm$ 1.7 g of soil was packed in each column (n = 4). After packing, columns were equilibrated by pumping artificial groundwater through them for 48 h using a multichannel peristaltic pump (ISM931C, Simatic® IPC, Germany).

2.4. Tracer tests

Estimations of hydrological parameters in each column were conducted using tracer tests after equilibration of the columns and before switching to PFAS-spiked water (Table S7 in SI). Sodium chloride (NaCl) was chosen as a conservative tracer at a starting molar concentration of 0.43 M. After equilibration of the columns, the inflow was switched to the tracer solution, which was pumped for ~24 h before the influent changed back to artificial groundwater. The flow rate was monitored through the tracer test and was steadily 288 mL d^{-1}. Effluent samples were taken every 50 min, starting at the same time as the tracer pulse, with the use of a fraction collector (CF-2 Fraction Collector, 115 V, Repligen), and the electrical conductivity of the aliquots was measured (Cond 3310 & TetraCon 325, WTW). Conductivity measurements were converted to molar concentrations of NaCl, using a 5-point calibration curve (R^2 > 0.99) (Figure S1 in SI). After sample collection and analysis, results from the tracer tests with NaCl were processed with the CXTFIT 2.0 code, embedded in Excel, which incorporates a solution of the 1-D convection-dispersion equation (CDE) as the transport model (Toride et al., 1995).

2.5. Preparation of feed solution and sample collection

Spiked artificial groundwater was prepared with solution chemistry resembling the sampling location's groundwater based on field measurements (Tables S8 and S9 in SI). Using the field data, a geochemical equilibrium model in VisualMINTEQ was developed to define the solution chemistry of the artificial feed water. The pH of the solution was adjusted to 7.7 with the addition of HCO$_3^-$, to simulate field conditions. The salts added to the feed solution and their concentrations can be seen in Table S10 in SI.

The feed solution was spiked with a total of 12 PFAS, including C4–C10 perfluorocarboxylic acids (PFCAs) (PFPeA, PFHxA, PFHpA, PFOA, PFNA, PFDA, PFUnDA), C4, C6, C8 perfluorosulfonic acids (PFSAs) (PFBS, PFHxS, PFOS), and 6:2 and 8:2 fluorotelomer sulfonic acids (FTSAs) (6:2 FTSA, 8:2 FTSA). The final total concentration was 0.87 mg L^{-1} for $\sum_{12}$PFAS, evenly distributed among individual PFAS (C = 67 μg L^{-1} for individual PFAS), corresponding to the high end of environmentally relevant concentrations for contaminated soils (Brusseau et al., 2020). The spiked feed solution was pumped through the columns at a flow rate of Q = 288 mL d^{-1}, ensuring a continuous upward flow and keeping saturated conditions. After approximately 400 pore volumes (PV), the inflow was switched from spiked to non-contaminated

artificial groundwater to test the desorption potential of PFAS from the soil. The duration of the whole experiment was approximately 150 days, or 596 PV.

PFAS concentrations were quantified for water outflow samples, as well as in segments of the soil columns. Sacrificial samples of the outflow water were taken at various times during the duration of the experiments (approximately every three days). After completion of the experiment, the soil columns were cut into five layers, to analyse soil concentration of PFAS for mass balance calculation.

2.6. PFAS analysis

PFAS analysis was conducted with the use of ultra high-performance liquid chromatography coupled with tandem mass spectrometry (UHPLC-MS/MS, Quantiva TSQ; Thermo Fischer Scientific, USA) through direct injection of water samples and solid-liquid extraction of soil samples (for details, see elsewhere (Ahrens et al., 2009)). Briefly, nine isotopically labelled internal standards (ISs) were used for PFAS quantitation ($^{13}C_4$-PFBA, $^{13}C_2$-PFHxA, $^{13}C_4$-PFOA, $^{13}C_5$-PFNA, $^{13}C_2$-PFDA, $^{13}C_2$-PFUnDA, $^{13}C_2$-PFDoDA, $^{18}O_2$-PFHxS, $^{13}C_4$-PFOS). Water samples were directly injected after methanol and IS addition, centrifugation (3000 rpm, 15 min), and filtration through a 0.45 μm recycled cellulose (RC) syringe filter fitted directly onto the syringe, producing aliquots of 1:1 methanol:water. Soil samples of 3 g were extracted twice with methanol and sodium hydroxide (NaOH), centrifuged, concentrated with N$_2$, and filtered through a 0.45 μm RC filter. The IS in soil samples was added before solvent extraction, to account for extraction losses. Negative blanks (n = 2) and positive control samples (n = 2) were included in the analysis. The positive controls were used as a reference to starting concentrations. The average recovery of ISs was 104% $\pm$ 5.2% for the water samples and 91% $\pm$ 23% for the soil samples (Tables S11 and S12 in SI). The method detection limit (MDL) for each target PFAS was calculated as $MDL = mean_{blanks} + 3*\sigma_{blanks}$ when concentrations were found in the method negative blanks, or using the lowest point of a 9-point calibration curve (0.01–100 ng mL^{-1}) in the absence of blank concentrations (Table S13 in SI). The positive control analysis showed a deviation of -9.60% from the theoretical spiked PFAS concentrations, which can be attributed to losses in the preparation and storage of spiking solutions or sorption of PFAS to the tube walls and other equipment that the inlet solution came in contact with.
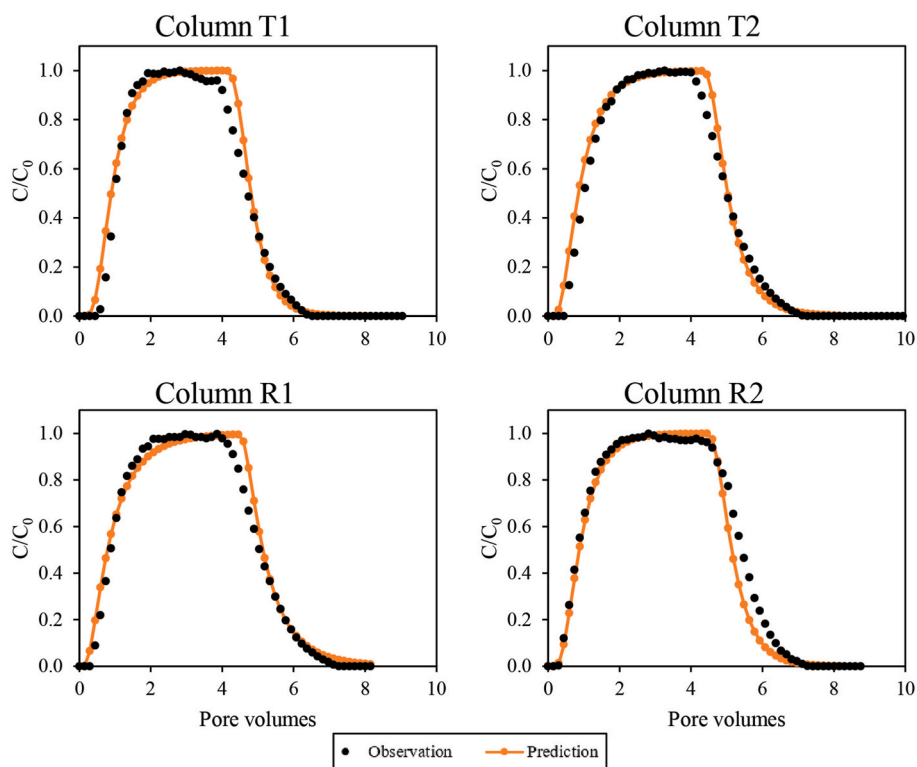
2.7. Organic carbon analysis

Organic carbon content was determined for reference and treated soil along the five layers of the soil columns to evaluate the redistribution and washing out of CAC in the columns. Soil samples of each layer were analysed for each column (Table S14 in SI). The carbon content and nitrogen content in the soils were determined through dry combustion according to ISO10694 (1995) and ISO 13878 (1998), respectively, using an elemental analyser for macrosamples (TruMac® CN, Leco corp, S:t Joseph, MI, USA). In short, the samples were combusted in a stream of pure O$_2$ at a temperature of 1350 °C, converting all carbon and nitrogen present in the sample to CO$_2$ and NO$_x$, respectively. In two separate runs, each sample's total carbon (TC) and total inorganic carbon (TIC) contents were determined. The total organic carbon (TOC) content was then calculated as TOC (%) = TC (%) - TIC (%).

3. Results and discussion

3.1. Tracer tests

Breakthrough curves (BTCs) of experimental and modelled data are shown in Fig. 1. The shape of the BTCs and the calculated parameters were indicative of uniform packing of all columns. A complete breakthrough of NaCl was noticed slightly before 2 PV for all columns. The BTCs showed a relatively symmetrical shape, denoting an equilibrium

Table 1
Overview of experiments and operating conditions.

Column	Matrix	C$_{\sum 12PFAS}$	C$_{PFAS, individual}$	Flow rate	pH
T$_1$	Treated soil	0.87 (mg L^{-1})	67 (μg L^{-1})	288 (mL d^{-1})	7.7
T$_2$	(0.031% CAC)				
R$_1$	Reference				
R$_2$	(reference soil)				

Fig. 1. Observed data and fitted breakthrough curves (BTCs) of the tested treated (T1, T2) and reference columns (R1, R2) of tracer tests with NaCl. Predicted values are modelled with the CXTFIT code, incorporating the 1-D convection-dispersion equation.

state in all the columns. Hydrological parameters were calculated based on the CXTFIT code and are presented in Table S7 in SI. Longitudinal dispersivities were estimated to be $\lambda = 2.72 \pm 0.87$ cm (n = 4). Peclet numbers were estimated to be less than 10 for all columns. The curves' fit had an average $R^2 = 0.979 \pm 0.0041$ (n = 4). The average pore water velocity was estimated by taking the time to reach $C/C_0 = 50\%$ for the tracer, as $\bar{v} = 2.97 \pm 0.07\ cm\ hr^{-1}$ (n = 4).
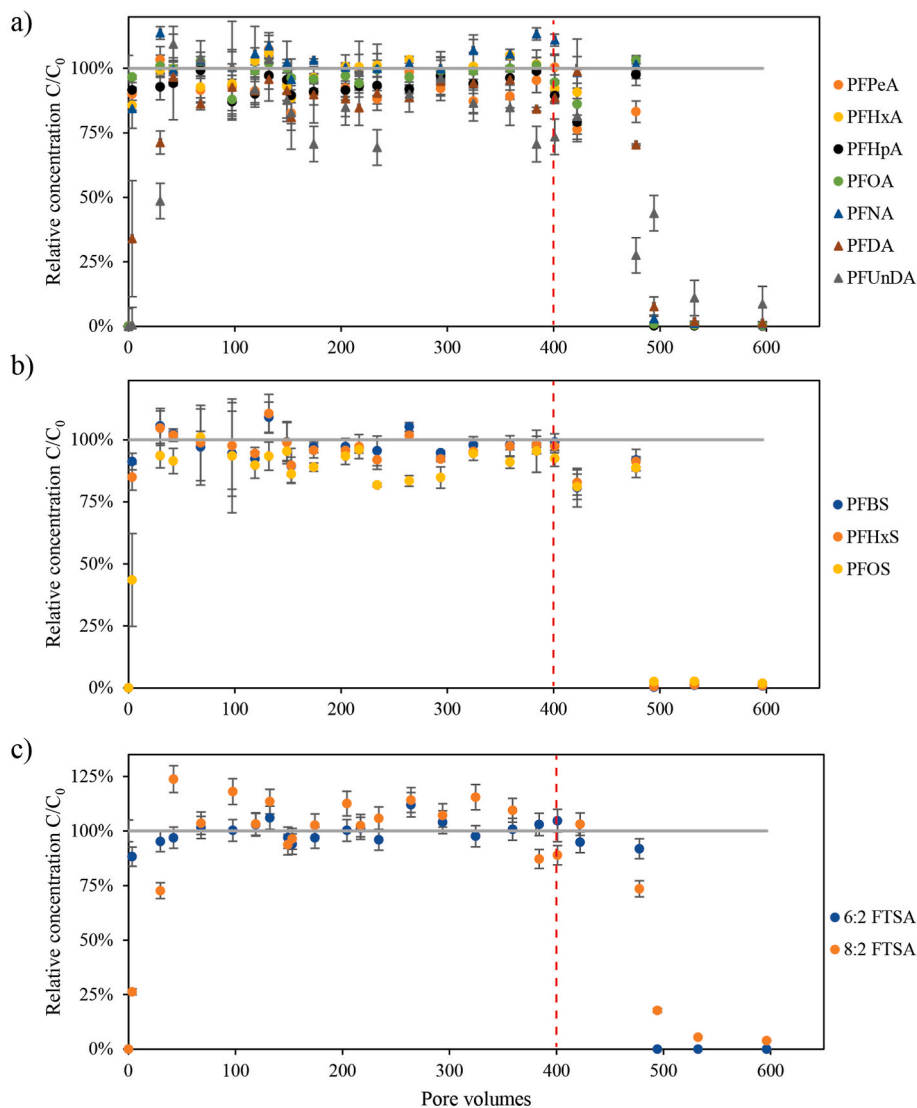
3.2. Column experiments

The leaching behaviour of PFAS differed between CAC-treated and reference soil columns (Figs. 2 and 3). Specifically, the breakthrough in treated soil columns (T1, T2) appeared much slower for many PFAS (Fig. 3) compared to reference soil columns (Fig. 2). Complete breakthrough for nearly all PFAS apart from PFNA and PFUnDA was noticed much faster in the reference soil (~30 PV) than in the treated soil (~233 PV), indicating an approximately eight times higher retardation for $\sum$PFAS in the treated soil. The tail of the BTCs showed similar behaviour for most PFAS. However, the drop of concentrations appeared steeper for the treated soil columns, indicating stronger adherence of PFAS to CAC than soil (Figure S2 in SI). In some instances, and especially in the starting samples for columns R1 and R2 (Fig. 2), effluent concentrations of PFAS were higher than the influent concentrations, resulting in C/C_0 > 1, thus showing an "overshoot" of concentrations. This effect has been previously described by other studies (McCleaf et al., 2017; Park et al., 2020) and can be attributed to chromatographic effects (i.e. PFAS leaching out at different time points) and the replacement of PFAS stored in the column when more hydrophobic PFAS (typically longer chain) arrive and compete for adsorption sites. Overshoot was more noticeable in PFCAs than PFSAs, confirming this theory, as PFCAs have lower hydrophobicity than their homologues (Higgins and Luthy, 2006). This is important to consider in field-scale applications since long-chain PFAS plumes can transport more slowly and thus induce a release of short-chain PFAS if they arrive at the treatment zone at a slower pace

and compete for sorption sites.

Marked differences were observed for individual PFAS depending principally on their perfluorocarbon chain length (BTCs for $\sum_{12}$PFAS and some individual PFAS can be seen in Figures S3 and S4 in SI). In the reference soil, an almost complete breakthrough (90%) was noticed immediately at the first sample (~3.5 PV) for C < 8 chain length PFAS, while PFUnDA (C = 10) exhibited the highest retardation, with a complete breakthrough at ~42.2 PV. PFOA showed a complete breakthrough at ~149 PV in treated soil, compared to ~30 PV in reference soil. In treated soil, some long-chain PFAS showed no complete breakthrough. Specifically, the longest chain PFCAs, PFDA and PFUnDA, had a maximum of 86% and 65% breakthrough, respectively, after 422 PV. For PFUnDA, there was also a delay in reaching maximum concentrations, with maximum concentrations being reached at 22 PV after the rest of the PFAS and while concentrations for the rest of PFAS were decreasing (Fig. 3). Therefore, there can be an increase in concentrations of long-chain PFAS even after switching to non-contaminated groundwater, indicating a delayed response to desorption. This phenomenon can be attributed to the lower transport rate of long-chain PFAS due to their lower solubility or to competition effects among PFAS for sorption sites, which can increase available sites for longer-chain PFAS when short-chain PFAS are not present in the solution (McCleaf et al., 2017). Micelle breakdown could also lead to increased concentrations for long-chain PFAS in the dissolved phase, however, the concentrations tested in this study were well below the critical micelle concentrations (Table S3 in SI) and micelle formation was unlikely. Conversely, short-chain PFAS exhibited a much faster breakthrough and a steeper decrease in concentrations after switching to non-contaminated groundwater (~400 PV). In field-scale scenarios flowrate fluctuations would also occur (e.g. due to heavy rainfall), resulting in desorption of shorter chain PFAS, as has been observed by Maizel et al. (2021), which would likely accentuate the increase of their concentration in the aqueous phase. The faster breakthrough of short-chain PFAS is important to consider in future treatment applications, due to the production
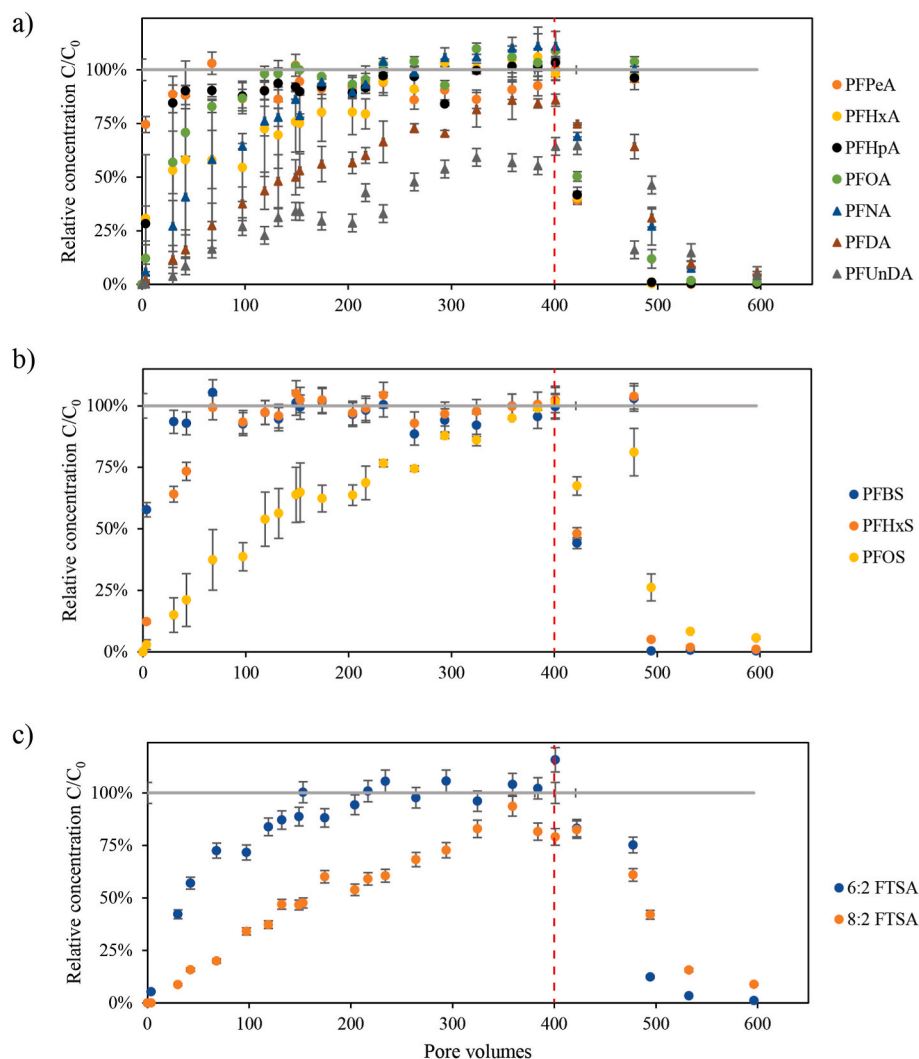
Fig. 2. Column breakthrough curves (BTCs) for a) PFCAs, b) PFSAs, and c) FTSAs in reference soil (columns R1, R2). C_0 corresponds to positive control concentrations. Error bars indicate methodological error as the standard deviation (n = 2). The red dashed line represents the time of switching to non-PFAS-spiked artificial groundwater. (For interpretation of the references to colour in this figure legend, the reader is referred to the Web version of this article.)

shift towards shorter-chained PFAS and the potential degradation of precursors, including FTSAs.
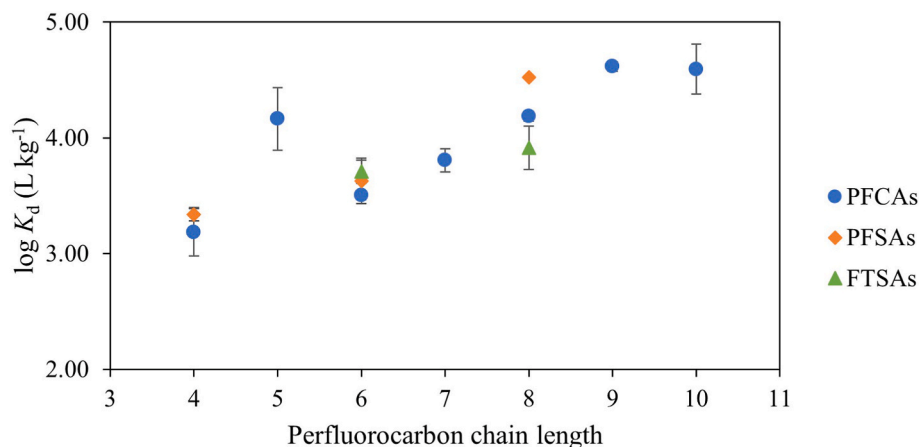
Comparing functional groups, PFCAs had slightly faster breakthroughs than both PFSAs and FTSAs, indicating stronger sorption for PFSAs and FTSAs than PFCAs. A similar trend has been noticed by Sorengard et al. (2019), who calculated K_d values for CAC based on batch tests. Differences based on the functional group were more noticeable in long-chain PFAS. Specifically, PFOS had a complete breakthrough at 400 PV, much later than its analogous PFNA, which showed a complete breakthrough at 234 PV. Stronger sorption of PFSAs than PFCAs has similarly been reported before for sorption to soils (Campos Pereira et al., 2018) and activated carbons (Park et al., 2020; Son et al., 2020). This can be explained by the stronger hydrophobicity of PFSAs than their analogous PFCAs due to the larger size of the sulphonate moiety (Higgins and Luthy, 2006). Higher experimental variability was noticed for PFCAs in treated soil, especially for short-chain ones (Fig. 3). This could be attributed to competition effects among PFAS, especially when the more hydrophobic longer-chain PFAS arrive and compete for sorption sites. Despite these experimental variations, the aforementioned trends are still noticeable.

3.3. Partitioning coefficients

Retardation of PFAS was calculated by comparing the BTCs of the tracer (Fig. 1) to the BTCs for individual PFAS (Figs. 2 and 3). Due to the fast breakthrough of some PFAS, a more accurate estimation of the retardation could be obtained by comparing the times for 80% breakthrough for PFAS to that of the tracer, as compared to doing this for 50% breakthrough times. Therefore, the time of 80% breakthrough was chosen, and the retardation factors were determined from $R_f = \frac{t_{80,NaCl}}{t_{80,PFAS}}$. Assuming linear adsorption, K_d values could subsequently be calculated as $K_d = (Rf - 1)*n_{eff}/\rho$, where Rf is the retardation factor calculated by the time required to reach $C/C_0 = 0.80$, n_{eff} is the effective porosity, and ρ is the bulk density of the packed soil (USEPA, 1999). The K_d coefficients ranged from $\sim 10^3$ to 10^5 L kg^{-1}, with a positive correlation between perfluorocarbon chain length and K_d for PFCAs, PFSAs, and FTSAs alike, increasing one order of magnitude from C_4 to C_{10} PFCAs (Fig. 4). The log K_d increased by 0.26, 0.32 and 0.20 log units for each CF_3 moiety for PFCAs, PFSAs and FTSAs, respectively. Comparing functional groups and the same perfluorocarbon chain length, the K_d for PFSAs was on average 0.05 log units higher compared to PFCAs (e.g. PFNA had $K_d = 14 \pm 1.4$ L g^{-1} versus $K_d = 30 \pm 0.27$ L g^{-1} for PFOS (C

Fig. 3. Column breakthrough curves (BTCs) for a) PFCAs, b) PFSAs, and c) FTSAs in CAC-treated soil (columns T1, T2). C_0 corresponds to positive control concentrations. Error bars indicate methodological error as the standard deviation (n = 2) The red dashed line represents the time of switching to non-PFAS-spiked artificial groundwater. (For interpretation of the references to colour in this figure legend, the reader is referred to the Web version of this article.)

Fig. 4. Average log partitioning coefficients between CAC-treated soil and aqueous phase (log K_d) for the AC fraction of the soil, as a function of perfluorocarbon chain length for PFCAs, PFSAs, and FTSAs. Error bars represent standard deviation of duplicate columns (n = 2).

= 8)). In contrast, no such trend of K_d values was observed for FTSAs compared to PFSAs or PFCAs. K_d values for the reference soil could not be determined for all PFAS, due to fast breakthrough (Figures S2 and S3

in SI). For those that K_d could be determined, values for CAC appeared to be 3–5 orders of magnitude higher than for the non-treated soil, which is in agreement when comparing with values reported in the literature for

natural soils (Milinovic et al., 2015). This indicates much stronger sorption to CAC than to soil, which can be attributed to the material's high surface area (900 m^2 g^{-1}) and small particle size (1–2 µm). The strong sorption despite the low ζ potential values of CAC (−80 to −2 mV) indicates that hydrophobic interactions likely govern the adsorption. This phenomenon has also been described by Du et al. (2014), who found it more pronounced for long-chain PFAS. However, interactions based on electrostatic effects cannot be excluded. Hansen et al. (2010) reported K_d values for GAC and PAC based on shaking tests, on the order of 10^3–10^5 for PAC and 10–10^2 for GAC, therefore the values calculated herein appear to be comparable to PAC and higher than GAC. The materials tested by Hansen et al. (2010) had similar iodine numbers and surface area, however, they consisted of larger particles (particle size 80% < 45 µm for PAC and 226 µm for GAC), which likely explains the noted differences. Specifically, a smaller particle size would lead to a larger micropore surface area, which can increase the adsorption capacity (Park et al., 2020). Sorengard et al. (2019) also derived K_d values for CAC-treated soil, which ranged between approximately 2–3.5 log units. The K_d values in this study are higher since they are based only on the CAC fraction of the treated soil (Fig. 4).

3.4. PFAS mass balance – soil concentrations

According to the PFAS analysis in the soil sections, treated soil columns retained a total of 13,000 µg kg^{-1} for $\sum$PFAS, versus 38 µg kg^{-1} for $\sum$PFAS for the reference soil, corresponding to 99.7% higher retention of PFAS in the treated soil columns after completion of the experiments. Additionally, the PFAS mass in the CAC-treated soil corresponds to 37 ± 5.04% of the total mass of $\sum$PFAS that was flushed through the columns during the experimental duration, indicating 63 ± 5.04% of $\sum$PFAS leached through the columns T1 and T2.

For the treated soil columns (T1, T2), the total mass of PFAS was primarily distributed within 6–15 cm from the inlet (82% ± 4.9%) and 33% ± 0.75% was concentrated at the last 3 cm of the column. The opposite was noticed for the reference columns (R1, R2), where they were mainly distributed close to the entrance point of the columns (42 ± 7.4% at 0–3 cm) (Fig. 5). Looking at the individual PFAS distribution in the treated soil (Figure S4 in SI), the same trend was noticed for most compounds, apart from PFUnDA, which mainly accumulated in the middle, and 6:2 FTSA, which was evenly distributed. In the same graph, it is also notable that the compound that accumulated the most is PFOS, along with long-chain PFCAs, i.e. PFUnDA, PFDA, and PFNA, while short-chain PFAS are present at much lower, almost undetectable concentrations. This is in accordance with the calculated K_d values, which
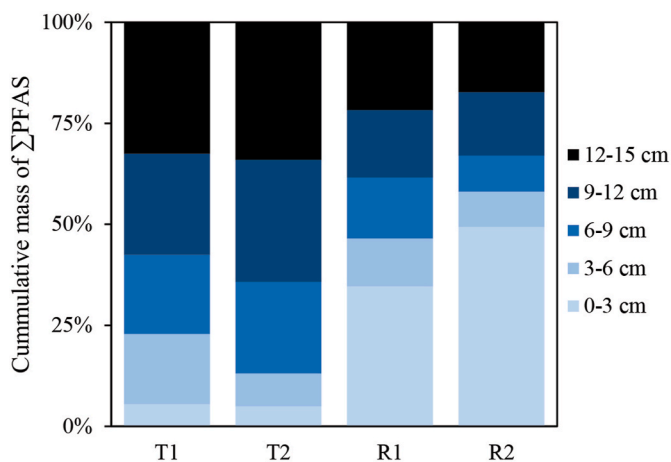
show that the adsorption coefficient is similar for these four PFAS (Fig. 4). The challenges for stabilisation of short-chain PFAS have been exhibited in other stabilisation applications, such as in pilot-scale S/S treatment (Sörengård et al., 2021) and treatment of drinking water with GAC filters (McCleaf et al., 2017). The effect of higher concentrations in the outlet for columns T1 and T2 was attributed to the transport of CAC within the soil matrix during the experiments, which is discussed in Section 3.5. Specifically, the low PFAS mass close to the inlet of the treated columns was expected to be due to depletion of CAC from the inlet and its deposition close to the outlet. In the reference soil columns (R1, R2), the cumulative mass gives a mechanistic understanding of PFAS fate in soils, indicating that they will transition to the next available site when available sorption sites are occupied and that the adsorption kinetics are relatively fast, considering the high flowrates of the experiments.

3.5. CAC distribution

During the equilibration of columns at the beginning of the experiments, CAC washout was noticed from the treated soil columns (T1, T2). This washout effect was quantified using TOC content analysis to estimate the lost carbon mass in treated soil (Fig. 6, Table S14 in SI). According to the TOC analysis, it was estimated that the treatment concentration of CAC was 0.031% in the treated soil. Further, the results suggested that 22% ± 8.4% of added CAC was eluted from the columns during the experiments, resulting in a final concentration of 0.024% CAC dry weight. It is worth noting that the transport of carbon particles was likely favoured by the relatively high pore water velocity and the short length of the columns. Lower velocities that would be found in realistic scenarios could enhance filtration of CAC, therefore leading to more carbon being attached to soil particles.

Complete depletion of CAC was noticed in the soil closer to the inlet (0–3 cm), whereas accumulation of CAC was detected in the soil closer to the outlet (12–15 cm from the inlet) (Fig. 6). This validated the results of the PFAS mass balance that indicated higher concentrations close to the outlet for columns T1, and T2 (Fig. 5). The calculations in this study, e.g. for K_d values, were based on the initial concentration of 0.031% since the timing of the CAC elution was uncertain.

4. Conclusions

The effectiveness of using colloidal activated carbon for PFAS soil treatment was demonstrated through column tests. Treatment of soil with an initial concentration of 0.031% w/w CAC resulted in an average of 8 times higher retardation of $\sum$PFAS transport compared to reference soil, despite 22% of CAC washing out during the experiments. For some long-chain PFAS (PFDA, PFUnDA), retardation was much higher, and breakthrough was never reached in treated soil during the experimental duration. Treatment efficiency was positively correlated with chain

Fig. 5. The cumulative mass of $\sum_{12}$PFAS across soil layers from the inlet (0–3 cm) to the outlet (12–15 cm) for columns T1, T2 (treated soil), and R1, R2 (reference soil).
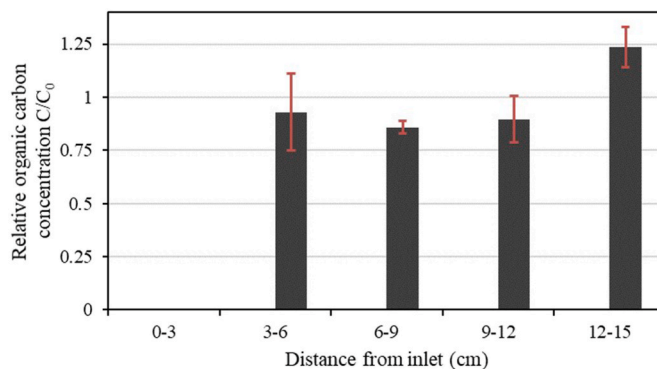

Fig. 6. Organic carbon distribution in the treated soil layers after completion of the experiments.

length, with long-chain PFAS exhibiting higher K_d values and functional group (PFSAs > PFCAs). The K_d values for CAC were in the range of 10^3–10^5 L kg^{-1}, and thus 3–5 orders of magnitude higher than the ones reported in the literature for soil. The mass balance analysis indicated a 37% retention of $\sum$PFAS of the total amount that was flushed through the treated columns. CAC washout was noticed during the experiments and, based on carbon analysis, was estimated to be 22% of the total carbon added to system. A certain degree of CAC mobility is considered necessary, to make sure it is well-distributed through all the flow channels of a soil matrix; however, CAC washout can also result in less effective treatment and even transport of PFAS to downstream locations. Further studies are therefore needed to fully understand the fate and transport of CAC in the subsurface.

Based on these data, treatment with CAC can result in significant retardation of PFAS, especially long-chain ones, and hinder their transport in the subsurface. While the treatment is not expected to last forever, it offers a promising solution when it comes to stabilisation efforts, chiefly due to its ease of application through injection in the subsurface. Re-injection of CAC post-treatment might be considered necessary when breakthrough is noticed in groundwater. Future research should focus on investigating further the transport of CAC and developing methods to improve its stability, avoiding elution of the material from the treated soil. Lastly, future experiments could focus on simulating more realistic conditions, for instance with the use of flow-interruption experiments.

Funding sources

Notes

The authors declare no competing financial interest.

Credit author statement

Georgios Niarchos: Conceptualization; Data curation; Formal analysis; Investigation; Methodology; Software; Project administration; Resources; Visualization; Validation; Writing – original draft; Writing – review & editing **Lutz Ahrens**: Conceptualization; Methodology; Writing – review & editing **Dan Berggren Kleja**: Conceptualization; Methodology; Writing – review & editing **Fritjof Fagerlund**: Funding acquisition; Conceptualization; Methodology; Writing – review & editing

Declaration of competing interest

The authors declare that they have no known competing financial interests or personal relationships that could have appeared to influence the work reported in this paper.

Data availability

Data will be made available on request.

Appendix A. Supplementary data

Supplementary data to this article can be found online at https://doi.org/10.1016/j.envpol.2022.119667.

References

Ahrens, L., Felizeter, S., Sturm, R., Xie, Z., Ebinghaus, R., 2009. Polyfluorinated compounds in waste water treatment plant effluents and surface waters along the River Elbe, Germany. Mar. Pollut. Bull. 58, 1326–1333. https://doi.org/10.1016/j.marpolbul.2009.04.028.

Ahrens, L., Norström, K., Viktor, T., Cousins, A.P., Josefsson, S., 2014. Stockholm Arlanda Airport as a source of per- and polyfluoroalkyl substances to water, sediment and fish. Chemosphere 129, 33–38. https://doi.org/10.1016/j.chemosphere.2014.03.136.

Baduel, C., Mueller, J.F., Rotander, A., Corfield, J., Gomez-Ramos, M.-J., 2017. Discovery of novel per- and polyfluoroalkyl substances (PFASs) at a fire fighting training ground and preliminary investigation of their fate and mobility. Chemosphere 185, 1030–1038. https://doi.org/10.1016/j.chemosphere.2017.06.096.

Banzhaf, S., Hebig, K.H., 2016. Use of column experiments to investigate the fate of organic micropollutants - a review. Hydrol. Earth Syst. Sci. 20, 3719–3737. https://doi.org/10.5194/HESS-20-3719-2016.

Bergström, S., 2014. Transport of Per- and Polyfluoroalkyl Substances in Soil and Groundwater in Uppsala. Sweden.

Bolan, N., Sarkar, B., Yan, Y., Li, Q., Wijesekara, H., Kannan, K., Tsang, D.C.W., Schauerte, M., Bosch, J., Noll, H., Ok, Y.S., Scheckel, K., Kumpiene, J., Gobindlal, K., Kah, M., Sperry, J., Kirkham, M.B., Wang, H., Tsang, Y.F., Hou, D., Rinklebe, J., 2021. Remediation of poly- and perfluoroalkyl substances (PFAS) contaminated soils – to mobilize or to immobilize or to degrade? J. Hazard Mater. 401, 123892 https://doi.org/10.1016/J.JHAZMAT.2020.123892.

Bräunig, J., Baduel, C., Heffernan, A., Rotander, A., Donaldson, E., Mueller, J.F., 2017. Fate and redistribution of perfluoroalkyl acids through AFFF-impacted groundwater. Sci. Total Environ. 596–597, 360–368. https://doi.org/10.1016/J.SCITOTENV.2017.04.095.

Brusseau, M.L., Anderson, R.H., Guo, B., 2020. PFAS concentrations in soils: background levels versus contaminated sites. Sci. Total Environ. 740, 140017 https://doi.org/10.1016/j.scitotenv.2020.140017.

Buck, R.C., Franklin, J., Berger, U., Conder, J.M., Cousins, I.T., de Voogt, P., Jensen, A.A., Kannan, K., Mabury, S.A., van Leeuwen, S.P., 2011. Perfluoroalkyl and polyfluoroalkyl substances in the environment: terminology, classification, and origins. Integrated Environ. Assess. Manag. 7, 513–541. https://doi.org/10.1002/ieam.258.

Campos Pereira, H., Ullberg, M., Kleja, D.B., Gustafsson, J.P., Ahrens, L., 2018. Sorption of perfluoroalkyl substances (PFASs) to an organic soil horizon – effect of cation composition and pH. Chemosphere 207, 183–191. https://doi.org/10.1016/J.CHEMOSPHERE.2018.05.012.

D'Agostino, L.A., Mabury, S.A., 2014. Identification of novel fluorinated surfactants in aqueous film forming foams and commercial surfactant concentrates. Environ. Sci. Technol. 48, 121–129. https://doi.org/10.1021/es403729e.

Dombrowski, P.M., Kakarla, P., Caldicott, W., Chin, Y., Sadeghi, V., Bogdan, D., Barajas-Rodriguez, F., Chiang, S.-Y., Dora, 2018. Technology review and evaluation of different chemical oxidation conditions on treatability of PFAS. Remed. J. 28, 135–150. https://doi.org/10.1002/REM.21555.

Du, Z., Deng, S., Bei, Y., Huang, Q., Wang, B., Huang, J., Yu, G., 2014. Adsorption behavior and mechanism of perfluorinated compounds on various adsorbents-A review. J. Hazard Mater. 274, 443–454. https://doi.org/10.1016/j.jhazmat.2014.04.038.

Filipovic, M., Laudon, H., McLachlan, M.S., Berger, U., 2015. Mass balance of perfluorinated alkyl acids in a pristine boreal catchment. Environ. Sci. Technol. 49, 12127–12135. https://doi.org/10.1021/ACS.EST.5B03403.

Gibert, O., Hernández Amphos, M., Vilanova, E., Cornellà, O., Wefer-Roehl, A., Kübeck, C., 2012. Guidelining Protocol for Soil-Column Experiments Assessing Fate and Transport of Trace Organics.

Guelfo, J.L., Wunsch, A., McCray, J., Stults, J.F., Higgins, C.P., 2020. Subsurface transport potential of perfluoroalkyl acids (PFAAs): column experiments and modeling. J. Contam. Hydrol. 233, 103661 https://doi.org/10.1016/j.jconhyd.2020.103661.

Hansen, M.C., Børresen, M.H., Schlabach, M., Cornelissen, G., 2010. Sorption of perfluorinated compounds from contaminated water to activated carbon. J. Soils Sediments 10, 179–185. https://doi.org/10.1007/S11368-009-0172-Z/TABLES/4.

Hearon, S.E., Orr, A.A., Moyer, H., Wang, M., Tamamis, P., Phillips, T.D., 2022. Montmorillonite clay-based sorbents decrease the bioavailability of per- and polyfluoroalkyl substances (PFAS) from soil and their translocation to plants. Environ. Res. 205, 112433 https://doi.org/10.1016/J.ENVRES.2021.112433.

Higgins, C.P., Luthy, R.G., 2006. Sorption of Perfluorinated Surfactants on Sediments. https://doi.org/10.1021/ES061000N.

Hoffman, K., Webster, T.F., Bartell, S.M., Weisskopf, M.G., Fletcher, T., Vieira, V.M., 2011. Private drinking water wells as a source of exposure to perfluorooctanoic acid (PFOA) in communities surrounding a fluoropolymer production facility. Environ. Health Perspect. 119, 92–97. https://doi.org/10.1289/EHP.1002503.

Høisæter, Å., Arp, H.P.H., Slinde, G., Knutsen, H., Hale, S.E., Breedveld, G.D., Hansen, M.C., 2021. Excavated vs novel in situ soil washing as a remediation strategy for sandy soils impacted with per- and polyfluoroalkyl substances from aqueous film forming foams. Sci. Total Environ. 794, 148763 https://doi.org/10.1016/J.SCITOTENV.2021.148763.

Høisæter, Å., Pfaff, A., Breedveld, G.D., 2019. Leaching and transport of PFAS from aqueous film-forming foam (AFFF) in the unsaturated soil at a firefighting training facility under cold climatic conditions. J. Contam. Hydrol. 222, 112–122. https://doi.org/10.1016/j.jconhyd.2019.02.010.

Huang, D., Xiao, R., Du, L., Zhang, G., Yin, L.S., Deng, R., Wang, G., 2021. Phytoremediation of poly- and perfluoroalkyl substances: a review on aquatic plants, influencing factors, and phytotoxicity. J. Hazard Mater. 418, 126314 https://doi.org/10.1016/J.JHAZMAT.2021.126314.

Huang, S., Jaffé, P.R., 2019. Defluorination of perfluorooctanoic acid (PFOA) and perfluorooctane sulfonate (PFOS) by acidimicrobium sp. strain A6. Environ. Sci. Technol. 53, 11410–11419. https://doi.org/10.1021/acs.est.9b04047.

Igor, T., Jean Noel, U., Jurate, K., Leo, W.Y.Y., 2021. Challenges in the PFAS remediation of soil and landfill leachate: a review, 2021 Adv. Environ. Eng. Res. 2. https://doi.org/10.21926/AEER.2102006. Page 1 2, 1–1.

Inyang, M., Dickenson, E.R.V., 2017. The use of carbon adsorbents for the removal of perfluoroalkyl acids from potable reuse systems. Chemosphere 184, 168–175. https://doi.org/10.1016/j.chemosphere.2017.05.161.

Kupryianchyk, D., Hale, S., Zimmerman, A.R., Harvey, O., Rutherford, D., Abiven, S., Knicker, H., Schmidt, H.P., Rumpel, C., Cornelissen, G., 2016. Sorption of hydrophobic organic compounds to a diverse suite of carbonaceous materials with emphasis on biochar. Chemosphere 144, 879–887. https://doi.org/10.1016/J.CHEMOSPHERE.2015.09.055.

Lewis, J., Sjöstrom, J., 2010. Optimizing the experimental design of soil columns in saturated and unsaturated transport experiments. J. Contam. Hydrol. 115, 1–13. https://doi.org/10.1016/j.jconhyd.2010.04.001.

Liu, M., Munoz, G., Vo Duy, S., Sauvé, S., Liu, J., 2022. Per- and polyfluoroalkyl substances in contaminated soil and groundwater at airports: a Canadian case study. Environ. Sci. Technol. 56, 885–895. https://doi.org/10.1021/ACS.EST.1C04798/SUPPL_FILE/ES1C04798_SI_002.XLSX.

Liu, Y., Li, X., Wang, X., Qiao, X., Hao, S., Lu, J., Duan, X., Dionysiou, D.D., Zheng, B., 2019. Contamination profiles of perfluoroalkyl substances (PFAS) in groundwater in the alluvial–pluvial plain of hutuo river, China. Water 11. https://doi.org/10.3390/W11112316, 2019 Page 2316 11, 2316.

Maizel, A.C., Shea, S., Nickerson, A., Schaefer, C., Higgins, C.P., 2021. Release of per- and polyfluoroalkyl substances from aqueous film-forming foam impacted soils. Environ. Sci. Technol. 55, 14617–14627. https://doi.org/10.1021/ACS.EST.1C02871/SUPPL_FILE/ES1C02871_SI_002.XLSX.

McCleaf, P., Englund, S., Östlund, A., Lindegren, K., Wiberg, K., Ahrens, L., 2017. Removal efficiency of multiple poly- and perfluoroalkyl substances (PFASs) in drinking water using granular activated carbon (GAC) and anion exchange (AE) column tests. Water Res. 120, 77–87. https://doi.org/10.1016/j.watres.2017.04.057.

McGregor, R., 2018. *In Situ* treatment of PFAS-impacted groundwater using colloidal activated Carbon. Remed. J. 28, 33–41. https://doi.org/10.1002/rem.21558.

Milinovic, J., Lacorte, S., Vidal, M., Rigol, A., 2015. Sorption behaviour of perfluoroalkyl substances in soils. Sci. Total Environ. 511, 63–71. https://doi.org/10.1016/J.SCITOTENV.2014.12.017.

Mukhopadhyay, R., Sarkar, B., Palansooriya, K.N., Dar, J.Y., Bolan, N.S., Parikh, S.J., Sonne, C., Ok, Y.S., 2021. Natural and engineered clays and clay minerals for the removal of poly- and perfluoroalkyl substances from water: state-of-the-art and future perspectives. Adv. Colloid Interface Sci. 102537 https://doi.org/10.1016/J.CIS.2021.102537.

Niarchos, G., Sörengård, M., Fagerlund, F., Ahrens, L., 2022. Electrokinetic remediation for removal of per- and polyfluoroalkyl substances (PFASs) from contaminated soil. Chemosphere 291, 133041. https://doi.org/10.1016/J.CHEMOSPHERE.2021.133041.

Nickerson, A., Rodowa, A.E., Adamson, D.T., Field, J.A., Kulkarni, P.R., Kornuc, J.J., Higgins, C.P., 2021. Spatial trends of anionic, zwitterionic, and cationic PFASs at an AFFF-impacted site. Environ. Sci. Technol. 55, 313–323. https://doi.org/10.1021/ACS.EST.0C04473/SUPPL_FILE/ES0C04473_SI_001.PDF.

Park, M., Wu, S., Lopez, I.J., Chang, J.Y., Karanfil, T., Snyder, S.A., 2020. Adsorption of perfluoroalkyl substances (PFAS) in groundwater by granular activated carbons: roles of hydrophobicity of PFAS and carbon characteristics. Water Res. 170, 115364 https://doi.org/10.1016/J.WATRES.2019.115364.

Place, B.J., Field, J.A., 2012. Identification of novel fluorochemicals in aqueous film-forming foams used by the US military. Environ. Sci. Technol. 46, 7120–7127. https://doi.org/10.1021/ES301465N/SUPPL_FILE/ES301465N_SI_001.PDF.

Qian, J., Shen, M., Wang, P., Wang, C., Li, K., Liu, J., Lu, B., Tian, X., 2017. Perfluorooctane sulfonate adsorption on powder activated carbon: effect of phosphate (P) competition, pH, and temperature. Chemosphere 182, 215–222. https://doi.org/10.1016/j.chemosphere.2017.05.033.

Rankin, K., Mabury, S.A., Jenkins, T.M., Washington, J.W., 2016. A North American and global survey of perfluoroalkyl substances in surface soils: distribution patterns and mode of occurrence. Chemosphere 161, 333–341. https://doi.org/10.1016/J.CHEMOSPHERE.2016.06.109.

Ross, I., McDonough, J., Miles, J., Storch, P., Thelakkat Kochunarayanan, P., Kalve, E., Hurst, J., Dasgupta, S.S., Burdick, J., 2018. A review of emerging technologies for remediation of PFASs. Remed. J. 28, 101–126. https://doi.org/10.1002/rem.21553.

Senevirathna, S.T.M.L.D., Mahinroosta, R., Li, M., KrishnaPillai, K., 2021. In situ soil flushing to remediate confined soil contaminated with PFOS- an innovative solution for emerging environmental issue. Chemosphere 262, 127606. https://doi.org/10.1016/J.CHEMOSPHERE.2020.127606.

Sepulvado, J.G., Blaine, A.C., Hundal, L.S., Higgins, C.P., 2011. Occurrence and fate of perfluorochemicals in soil following the land application of municipal biosolids. Environ. Sci. Technol. 45, 8106–8112. https://doi.org/10.1021/ES103903D.

Smith, M., Cross, K., Paden, M., Laban, P., 2016. Spring - Managing Groundwater Sustainably. IUCN, Gland, Switzerland. https://doi.org/10.2305/IUCN.CH.2016.WANI.8 en.

Son, H., Kim, T., Yoom, H.-S.S., Zhao, D., An, B., 2020. The adsorption selectivity of short and long per- and polyfluoroalkyl substances (PFASs) from surface water using powder-activated carbon. Water 12. https://doi.org/10.3390/W12113287, 2020 Page 3287 12, 3287.

Sörengård, M., Gago-Ferrero, P., Kleja, D.B., Ahrens, L., 2021. Laboratory-scale and pilot-scale stabilization and solidification (S/S) remediation of soil contaminated with per- and polyfluoroalkyl substances (PFASs). J. Hazard Mater. 402, 123453 https://doi.org/10.1016/j.jhazmat.2020.123453.

Sorengard, M., Kleja, D.B., Ahrens, L., 2019. Stabilization of per- and polyfluoroalkyl substances (PFASs) with colloidal activated carbon (PlumeStop®) as a function of soil clay and organic matter content. J. Environ. Manag. 249, 109345 https://doi.org/10.1016/j.jenvman.2019.109345.

Sörengård, M., Niarchos, G., Jensen, P.E., Ahrens, L., 2019. Electrodialytic per- and polyfluoroalkyl substances (PFASs) removal mechanism for contaminated soil. Chemosphere 232, 224–231. https://doi.org/10.1016/j.chemosphere.2019.05.088.

Sörengård, M., Östblom, E., Köhler, S., Ahrens, L., 2020. Adsorption behavior of per- and polyfluoralkyl substances (PFASs) to 44 inorganic and organic sorbents and use of dyes as proxies for PFAS sorption. J. Environ. Chem. Eng. 8, 103744 https://doi.org/10.1016/J.JECE.2020.103744.

Sørmo, E., Silvani, L., Bjerkli, N., Hagemann, N., Zimmerman, A.R., Hale, S.E., Hansen, C.B., Hartnik, T., Cornelissen, G., 2021. Stabilization of PFAS-contaminated soil with activated biochar. Sci. Total Environ. 763, 144034 https://doi.org/10.1016/J.SCITOTENV.2020.144034.

Toride, N., Leij, F.J., van Genuchten, M.T.T., 1995. The CXTFIT Code for Estimating Transport Parameters from Tracer Experiments. Riverside, CA. Version 2.1, Research Report No. 137.

USEPA, 1999. Understanding Variation in Partition Coefficient, Kd, Values Volume I: the Kd Model, Methods of Measurement and Application of Chemical Reaction Codes.

Van Glubt, S., Brusseau, M.L., Yan, N., Huang, D., Khan, N., Carroll, K.C., 2021. Column versus batch methods for measuring PFOS and PFOA sorption to geomedia. Environ. Pollut. 268, 115917 https://doi.org/10.1016/j.envpol.2020.115917.

Weber, A.K., Barber, L.B., LeBlanc, D.R., Sunderland, E.M., Vecitis, C.D., 2017. Geochemical and hydrologic factors controlling subsurface transport of poly- and perfluoroalkyl substances, cape cod, Massachusetts. Environ. Sci. Technol. 51, 4269–4279. https://doi.org/10.1021/ACS.EST.6B05573.

Yao, Y., Gao, B., Fang, J., Zhang, M., Chen, H., Zhou, Y., Creamer, A.E., Sun, Y., Yang, L., 2014. Characterization and environmental applications of clay–biochar composites. Chem. Eng. J. 242, 136–143. https://doi.org/10.1016/J.CEJ.2013.12.062.

Yong, Z.Y., Kim, K.Y., Oh, J.E., 2021. The occurrence and distributions of per- and polyfluoroalkyl substances (PFAS) in groundwater after a PFAS leakage incident in 2018. Environ. Pollut. 268, 115395 https://doi.org/10.1016/J.ENVPOL.2020.115395.

Zhao, Z., Xie, Z., Möller, A., Sturm, R., Tang, J., Zhang, G., Ebinghaus, R., 2012. Distribution and long-range transport of polyfluoroalkyl substances in the Arctic, Atlantic Ocean and Antarctic coast. Environ. Pollut. 170, 71–77. https://doi.org/10.1016/J.ENVPOL.2012.06.004.